The validation of new phase-dependent gait stability measures: a modeling approach

Jian Jin[1], Dinant Kistemaker[1], Jaap H. van Dieën[1], Andreas Daffertshofer[1,2], Sjoerd M. Bruijn[1,2,3]

[1]Department of Human Movement Sciences, Faculty of Behavioural and Movement Sciences, Vrije Universiteit Amsterdam and Amsterdam Movement Sciences, Amsterdam, The Netherlands.

[2] Institute of Brain and Behavior Amsterdam

[3]Orthopaedic Biomechanics Laboratory, Fujian Medical University, Quanzhou, Fujian, PR China

ABSTRACT

Identification of individuals at risk of falling is important when designing fall prevention methods. Current stability measures that estimate gait stability and robustness appear limited in predicting falls in older adults. Inspired by recent findings of phase-dependent local stability changes within a gait cycle, we used compass-walker models to test several phase-dependent stability metrics for their usefulness to predict gait robustness. These metrics are closely related to the often-employed maximum finite-time Lyapunov exponent and maximum Floquet multiplier. They entail linearizing the system in a rotating hypersurface orthogonal to the period-one solution, and estimating the local divergence rate of the swing phases and the foot strikes. We correlated the metrics with the gait robustness of two compass walker models with either point or circular feet to estimate their prediction accuracy. To also test for the metrics' invariance under coordinate transform, we represented the point-feet walker in both Euler-Lagrange and Hamiltonian canonical form. Our simulations revealed that for most of the metrics, correlations differ between models and also change under coordinate transforms, severely limiting the prediction accuracy of gait robustness. The only exception that consistently correlated with gait robustness is the divergence of foot strikes. These results admit challenges of using phase-dependent stability metrics as objective measure to quantify gait robustness.

1. Introduction

Falling is a major threat, especially for older adults. About one third of all adults older than 65 years fall at least once per year, often with serious injuries and fractures as consequences (Tinetti et al., 1988). Without a doubt, there is an urgent need to identify individuals at risk, in particular, when it comes to customizing fall prevention (Bloem et al., 2001). Various measures have been proposed to quantify the risk of falling in humans. Given the apparent relation to dynamic stability, the local divergence exponent (maximum finite-time Lyapunov exponent) (Dingwell & Cusumano, 2000) and the maximum Floquet multiplier (Hurmuzlu & Basdogan, 1994) are the first to mention. Lockhart & Liu (2008) and Toebes et al. (2012) suggested that the local divergence exponent may allow for discriminating fallers from non-fallers. Yet, fall prediction in elderly using this metric have an accuracy of 80% at best (Van Schooten et al., 2016).

Most stability measures are obtained by looking at either stride-to-stride deviations of an isolated point (e.g. heel-strike state), or average deviations over all phases of gait cycles. Humans, however, have phase-dependent gait stability as we display distinct responses to perturbations when applied at different phases of a gait cycle (Berger et al., 1984; Duysens et al., 1992). Estimating gait stability at an isolated point of or from an average over the gait cycle may thus fail. Norris et al. (2008) identified the phase-dependency in local stability using a 'simple' walking model, and Ihlen et al. (2012) reported intra-stride local stability variations in human gait. These observations and studies ascertained the potential for using phase-dependent local stability information to quantify gait stability.

While the term *gait stability* may be intuitively sound, it is often confused with *gait robustness*. Robustness can be operationalized as the maximum magnitude of perturbations that a walker can handle, while stability reveals whether or not a walker will return to its periodic motion after an infinitesimal perturbation. Infinitesimally implies locality (here close to a limit cycle). Stability, or better, *local stability*, does, in general, not relate to the maximum *size* of the perturbation that a non-linear system can handle, i.e. robustness. As such, the relation between a given stability metric and gait robustness is far from straightforward. Take the maximum Floquet multiplier as an example: It is a perfectly valid stability metric for periodic systems (Hurmuzlu & Moskowitz, 1987) but modeling (Bruijn et al., 2011; Hobbelen & Wisse, 2007; Su & Dingwell, 2007) as well as experimental studies (van Schooten et al., 2011) showed its limitations as proxy for gait robustness.

In a limit cycle system like a dynamic walker, locally stable phases and unstable phases may coexist. In that case, averaging local stability measures may lead to a loss of information regarding local stability tendencies. Perturbations applied during unstable phases may lead to larger deviations from the limit cycle than applied during stable phases. To address this, phase-dependent stability metrics have been introduced by Ali & Menzinger, (1999). By and large, they are based on a limit cycle's local stability quantified by the aforementioned responses to infinitesimal perturbations, but applied at different phases of the cycle. When it comes to human gait, phase-dependent stability metrics have, in fact, been shown to potentially improve the accuracy of fall prediction over cycle-averaged parameters (Ihlen et al., 2018).

The goal of the current study was to further validate phase-dependent stability measures for walking. Directly testing these stability measures on empirical data is hard, given the enormous complexity and variability of human walking. Therefore, rather than directly testing on empirical data, we asked: Can phase-dependent stability measures provide proper predictions of gait robustness in 'simple' walking models (Bruijn et al., 2013). A positive answer would render us more promise to apply this to empirical data and the negative answer would smother this hope. To answer our question, we devised several phase-dependent stability measures based on a two-dimensional compass walker model with point feet (Garcia, 1998; Goswami et al., 1998; Norris et al., 2008). To validate the different metrics, we determined their relations with the walker's gait robustness. We also tested whether these relations were stronger than those between the commonly used local divergence exponent and gait robustness. Next, we asked whether the corresponding results transferred to a slightly more complicated model including circular rather than point feet. Finally, we investigated the extent to which our phase-dependent stability metrics are invariant to changes in the coordinate system, in particular, when formulating the walker dynamics in either Hamiltonian canonical or Euler-Lagrange form. A dependency of the choice of coordinates would severely limit the usefulness of any measure for fall prediction in humans.

2. Methods

2.1 Models

Compass walker with point feet. The first model we incorporated is illustrated in Figure 1. It is a passive dynamic compass walker with point feet (Garcia, 1998; Norris et al., 2008). In brief, the model consists of two massless legs connecting the hip point mass M and foot point masses m; we denote the mass ratio as $\beta = m/M$. The state variables can be defined as $s =$

$(\theta, \varphi, \dot{\theta}, \dot{\varphi})^T$, where θ represents the angle of the stance leg with respect to the normal of the inclined plane, φ is the angle between the legs, and $\dot{\theta}$ as well as $\dot{\varphi}$ are the respective angular velocities. A gait cycle (one step) comprised a swing phase and an instantaneous double stance phase. At the double stance moment (= foot strike), we assumed a fully inelastic collision of the leading leg and exploited the conservation of angular momentum that here gives rise to a linear mapping from pre- to post-collision state. We let the model walk down a surface with slope γ. Throughout our paper we rescaled time by $\sqrt{l/g}$ to ease legibility.

A more detailed description including the Euler-Lagrange equations of motion can be found in *Appendix A*, which we adopted the notation of Garcia (1998) and Norris et al. (2008).

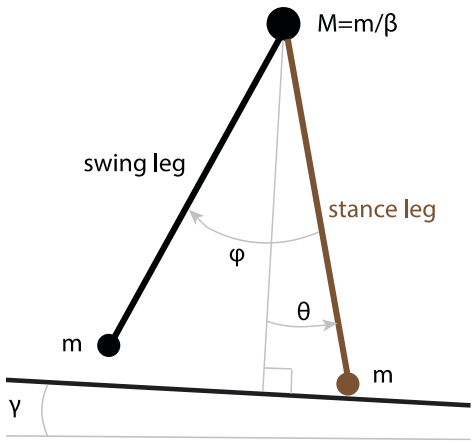

Figure 1. Compass walker model with point feet. This model consists of two massless legs connecting the hip point mass M and foot point masses m. θ is the angle of the stance leg with respect to the normal of the inclined plane and φ is the angle between the legs.

We also analyzed this compass walker model using Hamiltonian form. In that formulation, the state variables were defined as $s = (\theta, \varphi, p_\theta, p_\varphi)^T$, where p_θ and p_φ denote the canonical conjugate momenta with respect to θ and φ. The corresponding equations of motion can be found in *Appendix B*. In order to find the general relations between stability metrics and gait robustness of the model in later steps, we included a variety of configuration parameters by systematically varying the slope γ and mass ratio β ($\gamma = 10^{-3} \ldots 1.2 \cdot 10^{-2}$ in steps of $\Delta\gamma = 2 \cdot 10^{-4}$ and $\beta = 2 \cdot 10^{-3} \ldots 1 \cdot 10^{-1}$ in steps of $\Delta\beta = 2 \cdot 10^{-3}$), yielding $56 \times 50 = 2800$ parameter combinations.

Compass walker with circular feet. We also simulated a 2D compass walker model with circular feet. In this model, the state variables are $s = (\varphi_1, \varphi_2, \dot{\varphi}_1, \dot{\varphi}_2)^T$, where the definitions of these angles are given in Figure 2. More details of the configurations and equations of motions can be found in Wisse & Schwab, (2005). The circular feet walker also has instantaneous foot strike.

The foot radius r was varied as $r = 0.01 \ldots 0.49$ in steps of $\Delta r = 0.04$ and the slope γ were varied like for the point feet walker model yielding $13 \times 56 = 728$ parameter combinations.

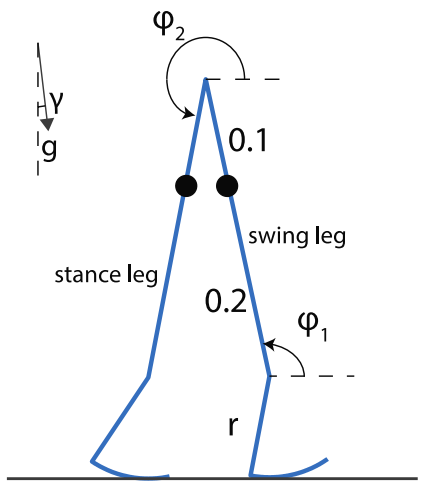

Figure 2. Circular feet compass walker and its configurations. A snapshot is captured at the end of a step. For simulation purposes, gravity was tilted to simulate an inclined slope γ. φ_1 and φ_2 are the angles of the swing leg and stance leg with respect to the inclined slope, r is the radius of the foot.

2.2 Numerical simulations

For the point feet walker we used a Runge-Kutta (4,5) integrator, while for the circular feet walker we followed Casius, et al., (2004) and employed an integrator for non-stiff differential equations; all simulations were realized in Matlab (The Mathworks, Natick, MA) . The absolute tolerance and relative tolerance were both 10^{-8} for the point feet walker and 10^{-10} for the circular feet walker. To avoid foot scuffing, foot strike detection condition was defined by constraining θ to be less than -0.05 radians for the point feet walker, and the swing leg to be in front of the stance leg and the inter-leg angle to be larger than 5 degrees for the circular feet walker.

For every parameter combination, we searched for a period-one solution (i.e. a solution where the states at the end of the step are the same as those at the beginning of the step) using the Newton-Raphson method (Wisse & Schwab, 2005). Whenever a period-one solution was detected, we determined the Floquet multipliers from the Poincaré map reflecting error multiplication factors from the step-to-step map following (Wisse & Schwab, 2005). We ignored all the unstable solutions in further calculations by removing all the solutions with a maximum absolute Floquet multiplier > 1.

2.3 Stability measures

2.3.1 Gait robustness

In order to assess the robustness of the model, we determined the maximal step-up and step-down perturbation the model could handle for every parameter combination. To this aim, the

walker started from its stable period-one solution after which, in the first step, we applied a one-time step-up/step-down floor height difference. We gradually increased this perturbation size (with precision up to 10^{-5} for the point feet walker and 10^{-4} for the circular feet walker) until, after the perturbation, the model was no longer able to complete 30 steps (which were empirically enough for the disturbance to be attenuated if the walker would not fall earlier).

2.3.2 The local divergence exponent

To determine the widely used *local divergence exponent* or short-term maximum finite-time Lyapunov exponent, we employed Rosenstein's algorithm (Rosenstein et al., 1993). In brief, per parameter combination, we performed 5 simulations of 200 steps where at each step a floor height variation was added (zero-centered Gaussian white noise with a standard deviation of $2 \cdot 10^{-5}$). The time series of full states of the model were the direct input of the Rosenstein's algorithm for constructing the corresponding state space. Then, we applied Rosenstein's algorithm (Bruijn, 2017; Rosenstein et al., 1993) to estimate the local divergence exponent for each of these simulations, and averaged over 5 simulations per configuration.

2.3.2 Phase-dependent stability measures

Swing phase. To quantify the swing phase local stability of our models, we assessed how their continuous dynamics, $\dot{s} = f(s)$, behaves in the presence of an infinitesimal perturbation $\delta(t)$. This behavior can be approximated by linearization using the (time-dependent[1]) Jacobian at every point along the period-one solution:

$$\dot{\delta}(\mathrm{t}) = J(\mathrm{t}) \cdot \delta(\mathrm{t}) \,. \tag{1}$$

The eigenvalues of $J(t)$ quantify the rate at which the system returns to (negative eigenvalue) or moves away from (positive eigenvalue) the period-one solution in the corresponding eigen-directions after infinitesimal perturbations. Here, we would like to add that these eigen-directions may be (partly) along the period-one solution. In that case, the eigenvalues belonging to these eigenvectors quantify how perturbations yield a phase shift. Since such phase shifts in our model do not result in moving away from the period-one solution, they do not affect stability of the period-one solution as a whole, and hence are non-relevant for gait stability or gait robustness. One can circumvent this by performing a coordinate transformation to obtain eigenvalues that belong to eigenvectors that are orthogonal to the period-one solution.

---

1 Although local stability is defined in terms of time, for a period-one solution this directly translates to phase.

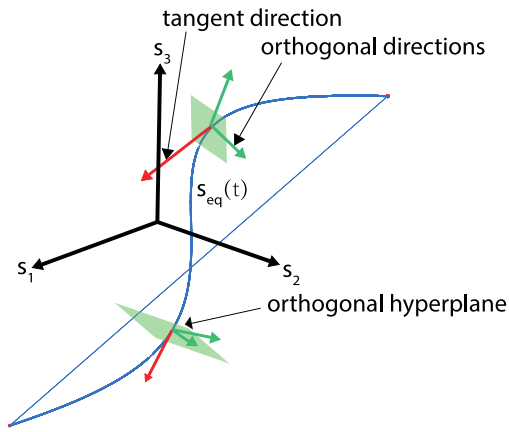

Figure 3. State space and moving coordinate frame. The period-one solution is displayed as the blue curve with a jump occurring at foot strike. We expressed our stability metrics in the orthogonal hyperplane since we are only interested in the eigenvalues that belong the eigenvectors that are orthogonal to the trajectory (i.e. the green arrows lying in the green plane), and can ignore eigenvalues that belong to eigenvectors that are along the period-one solution (i.e. red arrow).

Following Ali & Menzinger (1999); Norris et al. (2008), we used a moving coordinate frame $U(t)$, with one axis always remaining tangent to the period-one solution $f(s(t))^T \cdot \|f(s(t))\|^{-1}$, while the other axes span a hyperplane orthogonal to the period-one solution; cf. Fig. 3. One can use this moving coordinate frame to transform perturbations from the global frame $\delta(t)$ to the moving coordinate frame $\delta'(t)$ following

$$\delta'(t) = U(t) \cdot \delta(t)\,. \tag{2}$$

By taking the derivative of equation (2) with respect to time and using equation (1), one can obtain

$$\dot{\delta}'(t) = \left(U(t) \cdot J(t) \cdot U(t)^{-1} + \frac{dU(t)}{dt} \cdot U(t)^{-1}\right) \cdot \delta'(t) =: \bar{J}(t) \cdot \delta'(t)\,, \tag{3}$$

in which $\bar{J}(t)$ describes how perturbations evolve. However, due to our coordinate transform, the eigenvalues of $\bar{J}(t)$ are uncoupled. That is, the $\bar{J}(t)$ matrix obeys the form:

$$\bar{J}(t) = \begin{bmatrix} \lambda_{\parallel\parallel}(t) & \lambda_{\parallel\perp_1}(t) & \cdots \\ \lambda_{\perp_1\parallel}(t) & \lambda_{\perp_1\perp_1}(t) & \cdots \\ \vdots & \vdots & \ddots \end{bmatrix} \tag{4}$$

where vanishing $\lambda_{\perp_i\parallel}(t)$ imply that a tangent initial perturbation does not evolve onto the orthogonal hyperplane (Norris et al., 2008). Given that phase shifts do not alter stability in our model, one creates a reduced Jacobian matrix $J'(t)$ by removing the first column and top row of matrix $\bar{J}(t)$. The eigenvalues of $J'(t)$ describe the rate at which infinitesimal perturbations return to (negative eigenvalue) or move away (positive eigenvalue) from the period-one solution in the corresponding eigen-directions, which are all orthogonal to the direction of the period-one solution, i.e. they do not quantify a phase shift.

Figure 4 illustrates the evolution of all eigenvalues of the reduced Jacobian $J'(t)$ during the swing phase for the point feet walker. These eigenvalues indicate phase-dependent local stability orthogonal to the period-one solution, and one may derive potentially useful metrics from them. To do so, one can calculate the *trajectory-normal divergence rate*, $\Gamma(t)$, as the sum of all eigenvalues of $J'(t)$, indicating the mean contraction or expansion rate of all neighboring perturbations instead rather than along a single eigen-direction (Fig. 4 blue curve). From this trajectory-normal divergence rate, we calculated the following three metrics.

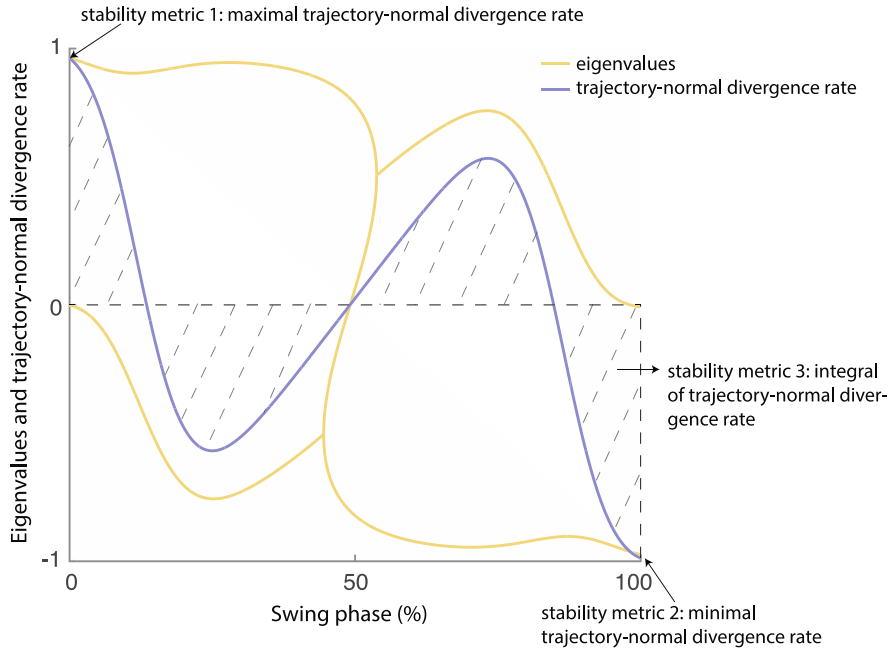

Figure 4. Eigenvalues and trajectory-normal divergence rate over the swing phase for the point feet walker. We indicate how the three stability metrics are derived from the trajectory-normal divergence rate (i.e. blue curve, obtained by taking the sum of all eigenvalues denoted in yellow curve). A similar figure could be made for the circular feet walker, but the shape of the curves will differ.

Stability metric i. The *maximum of trajectory-normal divergence rate* during the swing phase, i.e. $\max_{t \in Swing} \Gamma(t)$, quantifies the point with the largest trajectory-normal divergent rate in the swing phase. The higher the value, the more deviation an infinitesimal perturbation at this phase will yield from the orbit. Since it is a nonlinear system, it remains to be shown if for the walker models analyzed here, a higher value of this metric would result in a lower gait robustness.

Stability metric ii. The *minimum of the trajectory-normal divergence rate* during the swing phase or $\min_{t \in Swing} \Gamma(t)$ quantifies the point with smallest trajectory-normal divergent rate in the swing phase. The higher this value, the more deviation an infinitesimal perturbation at this phase will yield from the orbit; cf. metric *i* above.

Stability metric iii. The *integral over the trajectory-normal divergence rate* over the swing phase, $\int_{t \in Swing} \Gamma(t) dt$, provides the long-time multiplication factor of the volume all neighboring infinitesimal perturbations over the swing phase. Again, the higher this value, the more the infinitesimal perturbations will cause on average a deviation from the orbit. Note that this metric was also studied in the physics literature where it is known as the *trajectory-normal repulsion rate* ρ_T; it indicates the normal growth of infinitesimal normal perturbations to the trajectory over the time interval $[0, T]$ (Haller, 2011; Nave et al., 2019).

2.3.3 Foot strike and gait cycle

A complete gait cycle (one step) of the compass walkers contains a swing phase and an instantaneous double stance event (foot strike). Next to quantifying the local stability of the swing phase of the period-one solution of our models, we also quantified the local stability of the foot strike. We did this in a similar way as for the continuous dynamics. That is, we determined the Jacobian J_{FS} of the foot strike event. Its eigenvalues quantify the degree of deviation a perturbation may cause during the discrete event (i.e. absolute eigenvalue >1 indicate instability). Similar to the continuous case, where we eliminated the phase shift dimension before estimating the local divergence rate, we finally derived the *divergence* as product of all non-vanishing eigenvalues.

Stability metric iv. The *divergence of the reduced Jacobian of the foot strike*, div J'_{FS}, quantifies the multiplication factor of the volume of all infinitesimal perturbations surrounding the period-one solution before and after the foot strike event. The closer this metric is to zero, the more likely it is that the perturbations after foot strike is attenuated.

2.3.4 Floquet multipliers

Stability metric v. The *divergence of a full period-one solution* can be obtained by taking the absolute value of the product of all non-vanishing Floquet multipliers. Although it is known that the maximum Floquet multiplier is not an optimal proxy for gait robustness (van Schooten et al., 2011), the divergence of a gait cycle might be an alternative for further validation.[2]

[2] All code and data for this project can be found via the temporary link https://surfdrive.surf.nl/files/index.php/s/DK68NlvcEDGYaUu and will later be shared on zenodo.org).

3. Results

In order to evaluate how well these phase-dependent stability metrics and the local divergence exponent predict gait robustness, we correlated them with gait robustness (= maximum perturbation the model could handle) given our sets of parameter combinations. Before selecting our correlation measure, the general rubric for a "good correlation" maintains that: 1) for a given stability metric value, there should be a small variation in the corresponding gait robustness; 2) a monotonic increasing stability metric should be able to predict a monotonic decreasing (negative correlation) gait robustness. Two simple examples of a "good" and a "bad" correlation were illustrated in Figure 5 (panel B and E). Instead of using linear correlation coefficient which cannot quantify nonlinear associations, we used Kendall rank correlation as summarized in Table 1. This nonparametric correlation coefficient (between -1 and 1) evaluates the similarities in the ordering of the data when ranked by two variables, with 1 and -1 denoting perfect monotonic relationship between two variables in each direction.

Table 1. Kendall rank correlation coefficients of stability metrics with gait robustness for the different models and state space forms (subscript E refers to Euler-Lagrange and H to Hamilton). Green shading indicates negative correlations (higher stability metric value corresponding to lower robustness, as theoretically expected) and orange shading indicates positive correlations.

	local div. exponent	*metric i* max. div. rate	*metric ii* min. div. rate	*metric iii* div. swing ph.	*metric iv* div. foot strike	*metric v* div. gait cycle
model 1_E	-0.785	-0.471	-0.455	-0.969	-0.962	-0.245
model 2_E	-0.010	0.046	0.874	0.741	-0.797	0.572
model 1_H	-0.540	-0.930	0.614	-0.931	-0.962	-0.245

We illustrate this further in a series of figures, where we show the findings for the point feet walker (Fig. 5), the circular feet walker (Fig. 6), and provide a comparison between stability estimates for the point feet walker in Euler-Lagrange and Hamilton form (Fig. 7). For the point feet walker, two metrics (metric *iii* in panel D and metric *iv* in panel E) showed good correlations with gait robustness (Fig. 5), better than those of the local divergence exponent, suggesting that these phase-dependent stability metrics might be useful for predicting gait robustness. In particular, the divergence of swing phase (metric *iii*, the integral of the trajectory-normal divergence rate, panel E) and the divergence of foot strike (metric *iv*, panel F) showed extremely good correlations. However, for the circular feet walker model, the local divergence exponent and almost all of the phase-dependent stability metrics were not correlated well with gait robustness (Fig. 6). One exception was the minimal trajectory-normal divergence rate (metric *ii*, panel C) that, opposite to what we expected, was positively correlated with gait robustness. The inconsistent correlation directions of this metric (*ii*) cannot solely be explained

by the metric itself but probably stems from the nonlinearity of different models. Only the divergence of foot strike (metric *iv*, panel E) showed an acceptable correlation with gait robustness consistently. Comparing Figure 5 and Figure 6, the correlations between phase-dependent stability metrics and gait robustness highly depend on the model we considered; the prediction accuracy of gait robustness for phase-dependent stability metrics also cannot be preserved for two different models considered here, except the divergence of foot strike (metric *iv*, panel E).

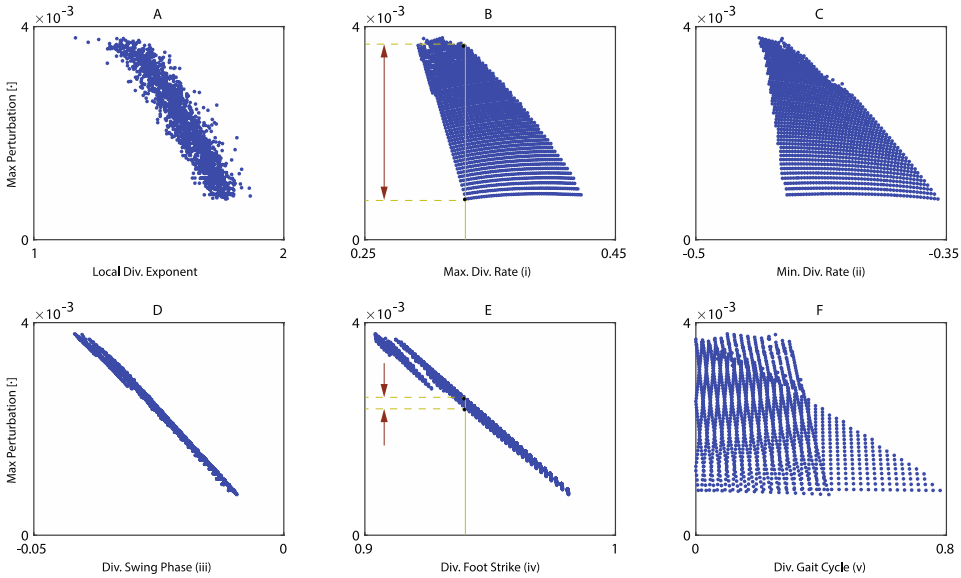

Figure 5. Relation between 1+5 stability metrics and gait robustness (maximum perturbation the model can handle for the point feet walker represented in Euler-Lagrange coordinates. Panel A represents the local divergence exponent, panels B to F represent phase-dependent stability metrics *i* to *v* respectively. Each data point represents one parameter combination of the model. Panel B and E give two examples of a "bad" and a "good" correlation. For a given value of stability metric, metric *i* predicts a wide range of maximum perturbation (bad), while metric *iv* predicts accurately only a small range of maximum perturbation (good).

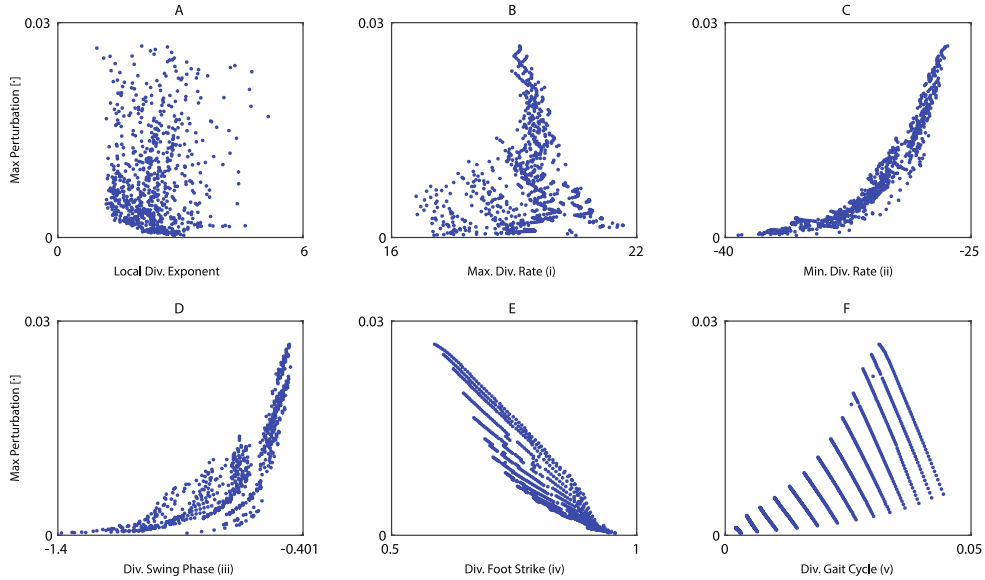

Figure 6. Relation between 1+5 stability metrics and gait robustness for the circular feet walker. Panel A represents the local divergence exponent, panels B to F represent phase-dependent stability metrics *i* to *v* respectively. Each data point represents one parameter combination of the model.

The influence of state space choice (here the Euler-Lagrange versus Hamilton form of the point-feet walker) on the correlations between our stability metrics and gait robustness is shown in Figure 7. Note that the maximal perturbations are independent of the state space choice. Furthermore, note that the panels E and F are necessarily the same for these two different coordinate systems. As can be readily seen from the figure, for the majority of metrics there was a clear dependency on the choice of coordinate system – see also *Appendix C* for more mathematical details. This means that the choice of the coordinate system (e.g. whether we choose angular velocity or angular momentum as our state variable) will affect the values of phase-dependent stability metrics and how well they correlate to gait robustness.

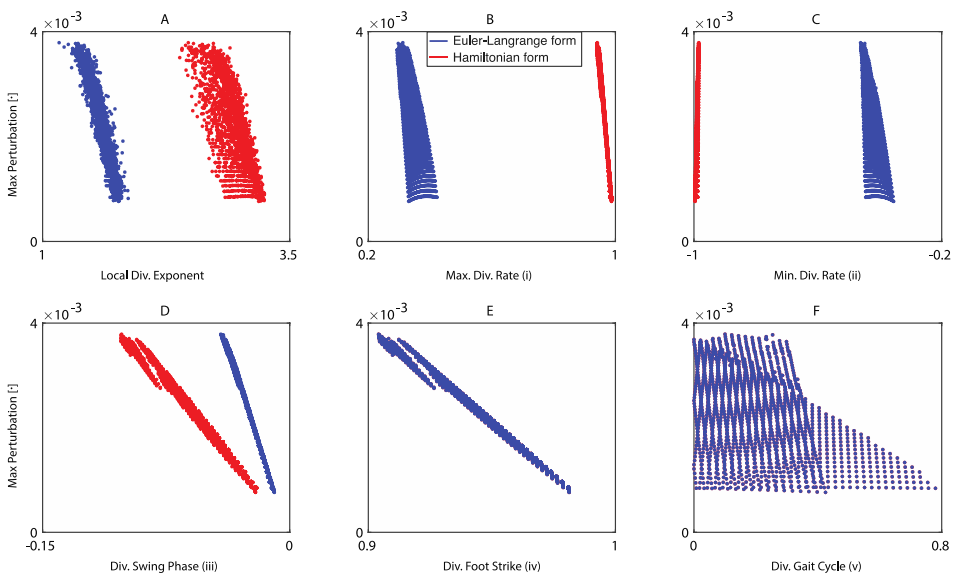

Figure 7. Comparing the relation between 1+5 stability metrics and gait robustness for the point feet walker in two different state space forms (red = Hamiltonian canonical form, blue = Euler-Lagrange form). the latter is identical to Figure 6 but the coordinates are scaled differently to highlight the difference with the outcomes in Hamiltonian form.

4. Discussion

We explored several phase-dependent stability measures, to assess if they may adequately and consistently predict robustness of simple walking models. To do so, we devised five phase-dependent stability metrics of compass walker models and investigated their correlations with gait robustness. We also calculated the commonly used local divergence exponent to test whether it may be outperformed by phase-dependent metrics. Our analysis revealed that some phase-dependent stability metrics could predict gait robustness better than the local divergence exponent for the simple walking model, but failed to predict gait robustness for the circular feet walker. It is worth mentioning that in Bruijn et al., (2012) the local divergence exponent was found to be well correlated with gait robustness of an arced feet walker with hip spring, but there the manipulated parameters were different (hip spring stiffness and foot radius) and were not changed simultaneously. Therefore, the correlations between stability measures and gait robustness also depend on which configuration parameters are varied.

Our results showed that the phase-dependent stability metrics depend on the state space form. This might be surprising, because the Lyapunov exponents are invariant to smooth coordinate transformation (Pikovsky & Politi, 2016). However, one has to realize that all phase-dependent stability metrics used here are *subspace* description of the original state space. They depend on the tangent vectors, which are not necessarily objective but may be coordinate- and norm-dependent. This may in fact be one of the reasons that different values of phase-dependent stability metrics are obtained when using different state variables or different scales of them. Similar arguments have been put forward by Nave et al., (2019) and Sternad et al., (2010). Interestingly, we also found the local divergence rate to be coordinate dependent, which is not a subspace description. We analyzed this in Appendix C.1 and found that due to the fact that the mass matrix is state-dependent, the coordinate transformation from angular velocities to Hamiltonian momenta is thus nonlinear. While we share the appeal in finding "objective" stability measures that are coordinate-invariant (more precisely, the measures that remained unchanged under any translation or rotation of reference frame), we must admit that formulating them is far beyond the scope of the current paper. Yet, we dare to suggest an alternative, namely to find the "best" state space representation, for instance using Hamiltonian canonical form or

action-angle coordinates (Arnold, 1978). However, this requires further studies that we leave for future work.

Only the divergence of foot strike appeared to be reasonably well related with gait robustness of our two walker models. Both of them have an instantaneous double stance phase. While this double stance phase is hardly comparable to that in humans, it is interesting to note that Ihlen et al. (2012) found that during heel strike, older adults had impaired gait stability compared to younger adults. Also, older fallers have been reported to have higher gait instability and a higher phase-dependent entropy around 0 and 60% (heel strike and toe-off) of the gait cycle (Ihlen et al., 2018; Ihlen et al., 2015). These findings do suggest that the stability of the foot strike could be of great importance in estimating/predicting gait robustness. A reason for that might be that (in our models) a dimension reduction occurs during foot strike, which constrains all post-impact perturbations in the state space into a 2D plane. Apparently, a stability metric derived in that plane can contain valuable information about a model's robustness.

The divergence of foot strike does seem to be a promising metric in particular when considering its consistent relation with gait robustness irrespective of coordinate choices and numerical settings. Yet, note that we calculated this metric directly from the analytical expression of the walker model. When working with empirical data, a different approach is needed, but our study may provide guidelines for this. One example, previously developed and applied to human data, is the method of Ihlen et al. (2012). And interesting alternative, introduced by Nave et al. (2019), is the trajectory divergence rate, which can be calculated from vector fields of data. In this context it is worth mentioning another potentially relevant metric of the trajectory-normal divergence rate, namely the *normal infinitesimal Lyapunov exponent*. It quantifies the instantaneous growth of perturbations transverse to the linearized trajectory, but has to the best of our knowledge not been applied to time series data yet. Finally, we would like to remark that there are of course also methods to calculate the entire Lyapunov spectrum in the presence of discontinuities, see for instance Müller, (1995), but supplemental numerical algorithms are far and few between and certainly not ready-for-use on empirical data. Moreover, since foot strike in human walking is not a discontinuity, it is still an open question whether such methods specifically designed for discontinuities should eventually be used.

Limitations of the current study. The phase-dependent stability metrics used here are based on the idea that perturbations tangent to the period-one solution do not affect stability of the gait and will only result in a phase shift along the unperturbed trajectory. This idea has widely been used in controller design in engineering, for example, transverse linearization (Shiriaev et al. ,

2008) and hybrid zero dynamics (Westervelt et al., 2007). However, in human locomotion, phase shift may play an important role, indeed. Stumbling perturbations applied at different phases can result in a phase reset to improve dynamic stability of gait (Yamasaki et al., 2003). Therefore, we also investigated the local divergence rate of the Jacobian $J(t)$ including both tangent and transverse local stability properties and found that the corresponding phase-dependent stability metrics also did not strongly correlate with gait robustness (data not presented here, but all the code and data can be accessed via the temporary link https://surfdrive.surf.nl/files/index.php/s/DK68NlvcEDGYaUu and will be shared on zenodo.org). Furthermore, we looked at the time-varying eigenvalue belonging to the eigenvector that is tangent to the period-one solution and found it to correlate only poorly with gait robustness.

We used passive dynamic walkers to investigate the relation between phase-dependent stability measures and maximum allowable perturbations of simple walking models. However, this may not be directly translated into the relation between stability measures and gait robustness of humans. For example, we found that our models could only handle very small step-up perturbations compared to the much larger step-down perturbations. This type of gait robustness is clearly not realistic in humans. Nevertheless, we still believe that the sum of step-up and step-down perturbation is a good representative of typical perturbations (e.g. a push or a pull in different phases of a gait cycle). On the one hand, Wisse et al., (2005) found that the step-down perturbation results in a larger stance leg velocity at the subsequent step. On the other hand, Chen et al., (2020) applied acceleration disturbances at five different phases of a gait cycle for a planar-feet walker model. They found that the Pearson correlation coefficient of the maximum allowable perturbations added at different phases were higher than 0.65 for all pairs and greater than 0.8 for most pairs. This suggests the measured maximum allowable perturbation (gait robustness) to be consistent along the gait cycle for simple walking models (Chen et al., 2020).

5. Conclusions

Phase-dependent stability measures have been advocated to characterize stability changes in compass walker models and in human gait. Our simulations revealed that they do not correlate with gait robustness in a consistent manner. In particular they may deviate strongly for different walker models and – arguably more important – they change with the choice of coordinate system. In our inventory, we encountered only a single phase-dependent metric, the divergence

of the double stance phase that displayed relatively good and coherent correlations with gait robustness. This almost linear relation, however, remains model dependent. It seems that phase-dependent stability measures and gait robustness in simple compass walker models are not one-to-one related, at least not the ones evaluated in the current study, which poses challenges for applying these metrics to empirical data.

Funding

SMB and JJ are funded by a VIDI grant (016.Vidi.178.014) from the Dutch Organization for Scientific Research (NWO).

Acknowledgements

The first author would like to thank Dr. Shane Ross for his helpful comments on the differences between state space coordinates.

References

Ali, F., & Menzinger, M. (1999). On the local stability of limit cycles. *Chaos: An Interdisciplinary Journal of Nonlinear Science*, *348*(9). https://doi.org/10.1063/1.166412

Arnold, V. I. (1978). *Mathematical Methods of Classical Mechanics*. *Advances in Mathematics*. https://doi.org/10.1007/978-1-4757-1693-1

Berger, W., Dietz, V., & Quintern, J. (1984). Corrective reactions to stumbling in man: neuronal co-ordination of bilateral leg muscle activity during gait. *The Journal of Physiology*. https://doi.org/10.1113/jphysiol.1984.sp015492

Bloem, B. R., Boers, I., Cramer, M., Westendorp, R. G., & Gerschlager, W. (2001). Falls in the elderly. I. Identification of risk factors. *Wiener Klinische Wochenschrift*, *113*(10), 352–362.

Bruijn, S. M. (2017). SjoerdBruijn/LocalDynamicStability. Zenodo. https://doi.org/http://doi.org/10.5281/zenodo.573285

Bruijn, S. M., Bregman, D. J. J., Meijer, O. G., Beek, P. J., & van Dieën, J. H. (2011). The validity of stability measures: A modelling approach. *Journal of Biomechanics*, *44*(13), 2401–2408. https://doi.org/10.1016/J.JBIOMECH.2011.06.031

Bruijn, S. M., Bregman, D. J. J., Meijer, O. G., Beek, P. J., & van Dieën, J. H. (2012). Maximum Lyapunov exponents as predictors of global gait stability: A modelling approach. *Medical Engineering and Physics*, *34*(4), 428–436. https://doi.org/10.1016/j.medengphy.2011.07.024

Bruijn, S. M., Meijer, O. G., Beek, P. J., & van Dieën, J. H. (2013). Assessing the stability of human locomotion: a review of current measures. *Journal of The Royal Society Interface*, *10*(83).

Casius, R., Bobbert, M., & van Soest, K. J. (2004). *Forward Dynamics of Two-Dimensional Skeletal Models. A Newton-Euler Approach*. *Journal of applied biomechanics* (Vol. 20). https://doi.org/10.1123/jab.20.4.421

Chen, T., Schmiedeler, J. P., & Goodwine, B. (2020). Robustness and efficiency insights from a mechanical coupling metric for ankle-actuated biped robots. *Autonomous Robots*. https://doi.org/10.1007/s10514-019-09893-w

Dingwell, J. B., & Cusumano, J. P. (2000). Nonlinear time series analysis of normal and pathological human walking. *Chaos: An Interdisciplinary Journal of Nonlinear Science*, *10*(4), 848. https://doi.org/10.1063/1.1324008

Duysens, J., Tax, A. A. M., Trippel, M., & Dietz, V. (1992). Phase-dependent reversal of reflexly induced movements during human gait. *Experimental Brain Research*. https://doi.org/10.1007/BF00227255

Garcia, M. (1998). The Simplest Walking Model: Stability, Complexity, and Scaling. *Journal of Biomechanical Engineering*, *120*(2), 281. https://doi.org/10.1115/1.2798313

Goswami, A., Thuilot, B., & Espiau, B. (1998). A study of the passive gait of a compass-like biped robot: Symmetry and chaos. *International Journal of Robotics Research*. https://doi.org/10.1177/027836499801701202

Haller, G. (2011). A variational theory of hyperbolic Lagrangian Coherent Structures. *Physica D: Nonlinear Phenomena*, *240*(7), 574–598. https://doi.org/10.1016/J.PHYSD.2010.11.010

Hobbelen, D. G. E., & Wisse, M. (2007). A disturbance rejection measure for limit cycle walkers: The gait sensitivity norm. *IEEE Transactions on Robotics*, *23*(6), 1213–1224. https://doi.org/10.1109/TRO.2007.904908

Hurmuzlu, Y., & Basdogan, C. (1994). On the Measurement of Dynamic Stability of Human Locomotion. *Journal of Biomechanical Engineering-Transactions of the Asme*. https://doi.org/10.1115/1.2895701

Hurmuzlu, Y., & Moskowitz, G. D. (1987). *Bipedal Locomotion Stabilized by Impact and Switching: II. Structural Stability Analysis of a Four-Element Model. Dynamics and Stability of Systems* (Vol. 2). https://doi.org/10.1080/02681118708806030

Ihlen, E. A. F., Goihl, T., Wik, P. B., Sletvold, O., Helbostad, J., & Vereijken, B. (2012). Phase-dependent changes in local dynamic stability of human gait. *Journal of Biomechanics*, *45*(13), 2208–2214. https://doi.org/10.1016/j.jbiomech.2012.06.022

Ihlen, E. A. F., van Schooten, K. S., Bruijn, S. M., van Dieën, J. H., Vereijken, B., Helbostad, J. L., & Pijnappels, M. (2018). Improved prediction of falls in community-dwelling older adults through phase-dependent entropy of daily-life walking. *Frontiers in Aging Neuroscience*. https://doi.org/10.3389/fnagi.2018.00044

Ihlen, E. A. F., Weiss, A., Helbostad, J. L., & Hausdorff, J. M. (2015). The Discriminant Value of Phase-Dependent Local Dynamic Stability of Daily Life Walking in Older Adult Community-Dwelling Fallers and Nonfallers. *BioMed Research International*. https://doi.org/10.1155/2015/402596

Lockhart, T. E. Te, & Liu, J. (2008). Differentiating fall-prone and healthy adults using local dynamic stability. *Ergonomics*, *51*(12), 1860–1872. https://doi.org/10.1080/00140130802567079.Differentiating

Müller, P. C. (1995). Calculation of Lyapunov exponents for dynamic systems with discontinuities. *Chaos, Solitons and Fractals*. https://doi.org/10.1016/0960-0779(94)00170-U

Nave, G. K., Nolan, P. J., & Ross, S. D. (2019). Trajectory-free approximation of phase space structures using the trajectory divergence rate. *Nonlinear Dynamics*. https://doi.org/10.1007/s11071-019-04814-z

Norris, J. A., Marsh, A. P., Granata, K. P., & Ross, S. D. (2008). Revisiting the stability of 2D passive biped walking: Local behavior. *Physica D: Nonlinear Phenomena*, *237*(23), 3038–3045. https://doi.org/10.1016/j.physd.2008.07.008

Pikovsky, A., & Politi, A. (2016). *Lyapunov exponents: A tool to explore complex dynamics*. Cambridge University Press.

Rosenstein, M. T., Collins, J. J., & De Luca, C. J. (1993). A practical method for calculating largest Lyapunov exponents from small data sets. *Physica D: Nonlinear Phenomena*, *65*(1–2), 117–134. https://doi.org/10.1016/0167-2789(93)90009-P

Shiriaev, A. S., Freidovich, L. B., & Manchester, I. R. (2008). Can we make a robot ballerina perform a pirouette? Orbital stabilization of periodic motions of underactuated mechanical systems. *Annual Reviews in Control*, *32*(2), 200–211. https://doi.org/10.1016/J.ARCONTROL.2008.07.001

Sternad, D., Park, S. W., Müller, H., & Hogan, N. (2010). Coordinate dependence of variability analysis. *PLoS Computational Biology*. https://doi.org/10.1371/journal.pcbi.1000751

Su, J. L.-S., & Dingwell, J. B. (2007). Dynamic Stability of Passive Dynamic Walking on an Irregular Surface. *Journal of Biomechanical Engineering*, *129*(6), 802. https://doi.org/10.1115/1.2800760

Tinetti, M. E., Speechley, M., & Ginter, S. F. (1988). Risk-factors for falls among elderly persons living in the community. *The New England Journal of Medicine*, *319*(26), 1701–1707.

Toebes, M. J. P., Hoozemans, M. J. M., Furrer, R., Dekker, J., & Van Dieën, J. H. (2012). Local dynamic stability and variability of gait are associated with fall history in elderly subjects. *Gait and Posture*, *36*(3), 527–531. https://doi.org/10.1016/j.gaitpost.2012.05.016

Van Schooten, K. S., Pijnappels, M., Rispens, S. M., Elders, P. J. M., Lips, P., Daffertshofer, A., … Van Dieën, J. H. (2016). Daily-life gait quality as predictor of falls in older people: A 1-year prospective cohort study. *PLoS ONE*. https://doi.org/10.1371/journal.pone.0158623

Van Schooten, K. S., Sloot, L. H., Bruijn, S. M., Kingma, H., Meijer, O. G., Pijnappels, M., & van Dieën, J. H.

(2011). Sensitivity of trunk variability and stability measures to balance impairments induced by galvanic vestibular stimulation during gait. *Gait & Posture*, *33*(4), 656–660. https://doi.org/10.1016/J.GAITPOST.2011.02.017

Westervelt, E., Grizzle, J. W., Christine, C., Ho Choi, J., & Morris, B. (2007). *Feedback Control of Dynamic Bipedal Robot Locomotion*. *Feedback Control of Dynamic Bipedal Robot Locomotion*.

Wisse, M., & Schwab, A. L. (2005). First Steps in Passive Dynamic Walking. In *Climbing and Walking Robots* (pp. 745–756). Berlin, Heidelberg: Springer Berlin Heidelberg.

Wisse, M., Schwab, A. L., van der Linde, R. Q., & van der Helm, F. C. T. (2005). How to keep from falling forward: Elementary swing leg action for passive dynamic walkers. *IEEE Transactions on Robotics*. https://doi.org/10.1109/TRO.2004.838030

Yamasaki, T., Nomura, T., & Sato, S. (2003). Phase reset and dynamic stability during human gait. *Biosystems*, *71*(1–2), 221–232. https://doi.org/10.1016/S0303-2647(03)00118-7

APPENDIX

A. Euler-Lagrange dynamics of the point feet walker

The gait cycle comprises of a swing phase and an instantaneous double stance phase yielding one step. At double stance (foot strike), we assume a fully inelastic collision of the leading leg and account for the conservation of angular momentum. The swing phase equations of motion can be readily derived from

$$\frac{d}{dt}\frac{\partial \mathcal{L}}{\partial \dot{q}} - \frac{\partial \mathcal{L}}{\partial q} = 0\,. \tag{A1}$$

The state q is given as $q = (\theta, \varphi)^T$ and $\mathcal{L}$ represents the Lagrangian. The corresponding equations of motion obey the form

$$\begin{aligned} M(\theta)\ddot{\theta} + N(\theta,\dot{\theta})\dot{\theta} + g(\theta) \\ = \begin{bmatrix} 1 + 2\beta - 2\beta\cos\varphi & \beta(\cos\varphi - 1) \\ \beta(\cos\varphi - 1) & \beta \end{bmatrix} \begin{bmatrix} \ddot{\theta} \\ \ddot{\varphi} \end{bmatrix} + \begin{bmatrix} 2\beta\dot{\varphi}\sin\varphi & -\beta\dot{\varphi}\sin\varphi \\ -\beta\dot{\theta}\sin\varphi & 0 \end{bmatrix} \begin{bmatrix} \dot{\theta} \\ \dot{\varphi} \end{bmatrix} \\ + \begin{bmatrix} -(1+\beta)\sin(\theta-\gamma)\,Mgl + \beta\sin(\theta-\varphi-\gamma)Mgl \\ \beta Mgl\sin(\varphi+\gamma-\theta) \end{bmatrix} = 0\,, \end{aligned} \tag{A2}$$

where $M(\theta)$ denotes the inertia matrix, $N(\theta,\dot{\theta})$ the Coriolis matrix, and $g(\theta)$ contains all gravitational forces. By defining the state as $s = (\theta, \varphi, \dot{\theta}, \dot{\varphi})^T$, one can rewrite the system (A2) in Euler-Lagrange form

$$\dot{s} = f_{EL}(s)\,. \tag{A3}$$

The foot strike occurs when the swing leg passes in front of the stance leg and hits the ground, that is, when $\cos\theta - \cos(\phi - \theta) = 0$ or simply $\phi - 2\theta = 0$ holds. To avoid foot scuffing we add $\theta < -0.05$ as additional, necessary condition. Then, foot strike collision is instant, and can be described by a linear operator from the pre-state (s^-) to the post-state (s^+):

$$s^+ = \begin{bmatrix} \theta \\ \varphi \\ \dot{\theta} \\ \dot{\varphi} \end{bmatrix}^+ = \begin{bmatrix} 1 & -1 & 0 & 0 \\ 0 & -1 & 0 & 0 \\ 0 & 0 & \dfrac{\cos 2\theta}{1+\beta\sin^2\varphi} & 0 \\ 0 & 0 & \dfrac{\cos 2\theta\,(1-\cos 2\theta)}{1+\beta\sin^2\varphi} & 0 \end{bmatrix} \begin{bmatrix} \theta \\ \varphi \\ \dot{\theta} \\ \dot{\varphi} \end{bmatrix}^- = G_{EL}(s^-)\,. \tag{A4}$$

B. Hamilton dynamics of the point feet walker

The swing phase dynamics can be given by four differential equations

$$\dot{s} = \begin{bmatrix} \dfrac{p_\theta + (1-\cos\varphi)p_\varphi}{1+\beta\sin^2\varphi} \\ \dfrac{p_\varphi + \beta(1-\cos\varphi)(p_\theta + 2p_\varphi)}{\beta(1+\beta\sin^2\varphi)} \\ -(1+\beta)\sin(\gamma-\theta) + \beta\sin(\gamma-\theta+\varphi) \\ \dfrac{4\beta\cos\varphi\sin\varphi\left[p_\varphi^2\left(\frac{1}{\beta} - 2\cos\varphi + 2\right) + p_\theta^2 - p_\varphi p_\theta(2\cos\varphi - 2)\right]}{(2\beta\sin^2\varphi+2)^2} - \dfrac{2p_\varphi^2\sin\varphi + 2p_\theta p_\varphi\sin\varphi}{2\beta\sin^2\varphi+2} - \beta\sin(\varphi+\gamma-\theta) \end{bmatrix} = f_H(s)\,, \tag{B1}$$

where the state is defined as $s = \left(\theta, \varphi, p_\theta, p_\varphi\right)^T$. We would like to note that this set of differential equations is different from those described in Norris et al. (2008), which contains an error in the term for p_φ.

As before, the foot strike collision is an instantaneous transition, described by a linear operator from the pre-state (s^-) to the post-state (s^+) that now reads:

$$s^+ = \begin{bmatrix} \theta \\ \varphi \\ p_\theta \\ p_\varphi \end{bmatrix}^+ = \begin{bmatrix} 1 & -1 & 0 & 0 \\ 0 & -1 & 0 & 0 \\ 0 & 0 & \dfrac{\cos\varphi}{1+\beta\sin^2\varphi} & \dfrac{\cos\varphi\,(1-\cos\varphi)}{1+\beta\sin^2\varphi} \\ 0 & 0 & 0 & 0 \end{bmatrix} \begin{bmatrix} \theta \\ \varphi \\ p_\theta \\ p_\varphi \end{bmatrix}^- = G_H(s^-)\,. \tag{B2}$$

C. Dependency on the coordinate system

C.1 Local divergence rate

In Cartesian coordinates, the generalized Hamiltonian momenta coincide with mechanical ones, i.e. the product of the inertia matrix and angular velocity:

$$p = \begin{bmatrix} p_\theta \\ p_\varphi \end{bmatrix} = M\dot{q} = \begin{bmatrix} 1 + 2\beta - 2\beta\cos\varphi & \beta(\cos\varphi - 1) \\ \beta(\cos\varphi - 1) & \beta \end{bmatrix} \begin{bmatrix} \dot{\theta} \\ \dot{\varphi} \end{bmatrix}. \tag{C1}$$

Taking the derivative of this equation gives

$$\begin{bmatrix} \dot{q} \\ \dot{p} \end{bmatrix} = \begin{bmatrix} 1 & 0 \\ \dot{M} & M \end{bmatrix} \begin{bmatrix} \dot{q} \\ \ddot{q} \end{bmatrix}. \tag{C2}$$

Let us write the Euler-Lagrange dynamics in state space form

$$\begin{aligned} \begin{bmatrix} \dot{q} \\ \ddot{q} \end{bmatrix} = f_{EL}(q,\dot{q}) &= \begin{bmatrix} 0 & I \\ f_{EL}^{21}(q,\dot{q}) & f_{EL}^{22}(q,\dot{q}) \end{bmatrix} \begin{bmatrix} q \\ \dot{q} \end{bmatrix} \\ &= \begin{bmatrix} 0 & I \\ f_{EL}^{21}(q,\dot{q}) & f_{EL}^{22}(q,\dot{q}) \end{bmatrix} \begin{bmatrix} I & 0 \\ 0 & M^{-1} \end{bmatrix} \begin{bmatrix} q \\ p \end{bmatrix}, \end{aligned} \tag{C3}$$

where I denotes the 2×2 identity matrix and 0 the 2×2 zero matrix and $f_{EL}^{21}(q,\dot{q})$ and $f_{EL}^{22}(q,\dot{q})$ are both 2×2 matrices. By combining (C2) and (C3), one can transform from Euler-Lagrange state space into Hamiltonian form (see also *Appendix B*):

$$\begin{bmatrix}\dot{q}\\ \dot{p}\end{bmatrix} = \begin{bmatrix}1 & 0\\ \dot{M} & M\end{bmatrix}\begin{bmatrix}0 & I\\ f_{EL}^{21}(q,\dot{q}) & f_{EL}^{22}(q,\dot{q})\end{bmatrix}\begin{bmatrix}I & 0\\ 0 & M^{-1}\end{bmatrix}\begin{bmatrix}q\\ p\end{bmatrix} = f_H(q,p). \tag{C4}$$

Since the system is conservative, the local divergence rate of $f_H(q,p)$ vanishes (Arnold, 1978), i.e. we have

$$\operatorname{div} f_H = \operatorname{trace}\left(\begin{bmatrix}1 & 0\\ \dot{M} & M\end{bmatrix}\begin{bmatrix}0 & I\\ f_{EL}^{21}(q,\dot{q}) & f_{EL}^{22}(q,\dot{q})\end{bmatrix}\begin{bmatrix}I & 0\\ 0 & M^{-1}\end{bmatrix}\right) = 0. \tag{C5}$$

Simplifying (C5) yields

$$\operatorname{div} f_{EL} = \operatorname{trace} f_{EL}^{22}(q,\dot{q}) = -\operatorname{trace}\left(M^{-1}\dot{M}\right) = -\frac{\beta \sin 2\phi}{1+\beta \sin^2\phi}\dot{\phi} \tag{C6}$$

which implies that local divergence rate, quantified by the sum of eigenvalues of the Jacobian matrix, are different for two sets of coordinates in the point feet walker. For Hamiltonian canonical coordinates, local divergence rate equals zero; for Euler-Lagrange coordinates, local divergence rate equals $-\frac{\beta \sin 2\phi}{1+\beta \sin^2\phi}\dot{\phi}$. This difference stems from the nonlinearity of the transformation $p = M\dot{q}$ as the inertia matrix M is state-dependent.

C.2 Phase-dependent stability metrics

Figure C1 shows a period-one solution $[s_1(t), s_3(t), s_4(t)]$ during swing phase in both Hamiltonian canonical form ($[\theta \quad p_\theta \quad p_\varphi]^T$) and Euler-Lagrange form ($[\theta \quad \dot{\theta} \quad \dot{\varphi}]^T$). The final state of the period-one trajectory p_φ in Hamiltonian canonical form is very close to zero. We found the relations between p_θ and $\dot{\theta}$ and between p_φ and $\dot{\varphi}$ to be almost linear: $\dot{\theta} \approx 0.994 p_\theta$ and $\dot{\varphi} \approx 24.1032 p_\varphi$. That is, a transforming from Hamiltonian to Euler-Lagrange coordinates may be approximate by keeping the scale of abcissa and rescaling ordinate by a factor of 24.

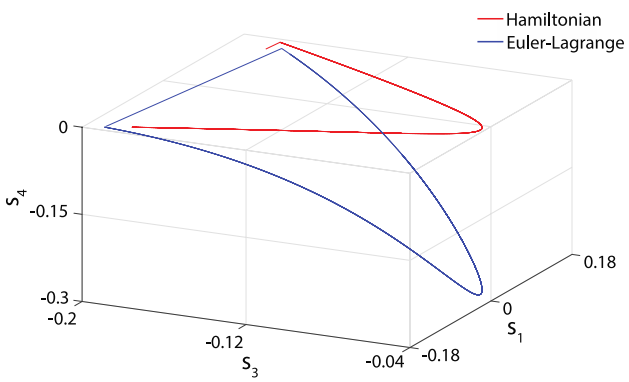

Figure C1. A period-one solution during swing phase in both Hamiltonian canonical form (red) and Euler-Lagrange form (blue).

In Figure C2 we illustrate the influence of coordinate transformation to the tangent and orthogonal vectors by sketching three sets of tangent/orthogonal vectors: one in Hamiltonian canonical coordinates (purple), one in Euler-Lagrange coordinates (green), and the other transformed from Euler-Lagrange to Hamiltonian canonical coordinates (yellow). Note that the transformed tangent vector is still parallel to the tangent vector in Hamiltonian coordinates, but the transformed orthogonal vector is no longer normal to the transformed tangent vector due to coordinate transformation. As a result, this type of coordinate transformation (scaling) makes our phase-dependent stability metrics dependent on the coordinate frame in which they are calculated. In other words, the derived phase-dependent stability metrics are only specific to particular coordinate choice or state space representation.

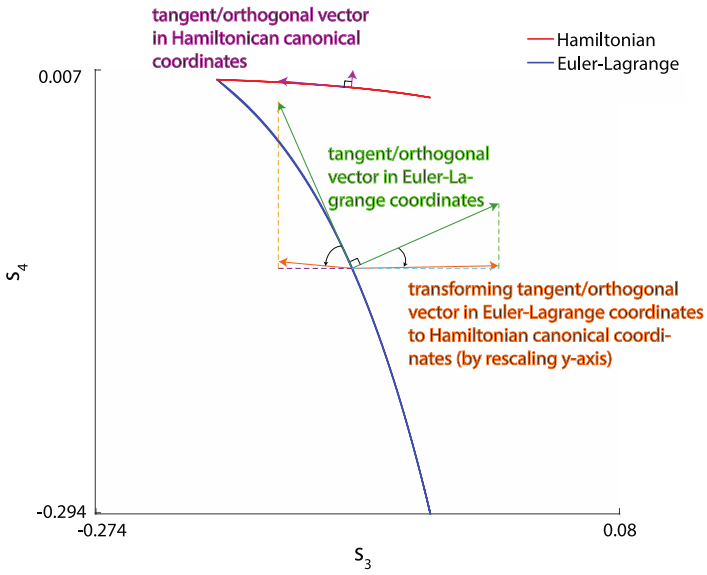

Figure C2. A period-one solution during swing phase in both Hamiltonian canonical form (red) and Euler-Lagrange form (blue). Three sets of tangent/orthogonal vectors are illustrated: in Hamiltonian canonical coordinates (purple), in Euler-Lagrange coordinates (green), transformed from Euler-Lagrange to Hamiltonian canonical coordinates (orange).

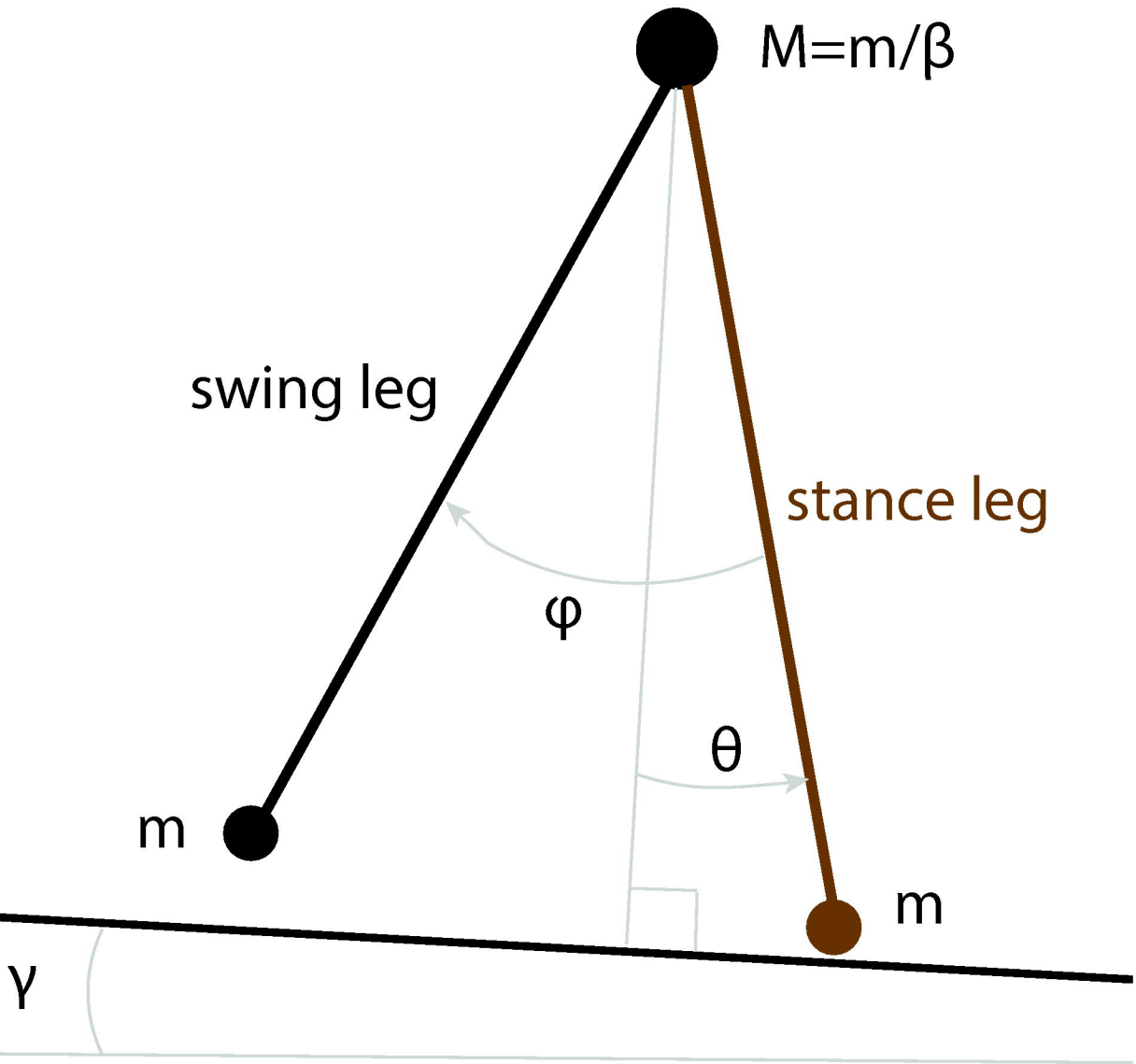
M=m/β
swing leg
stance leg
φ
θ
m
m
γ

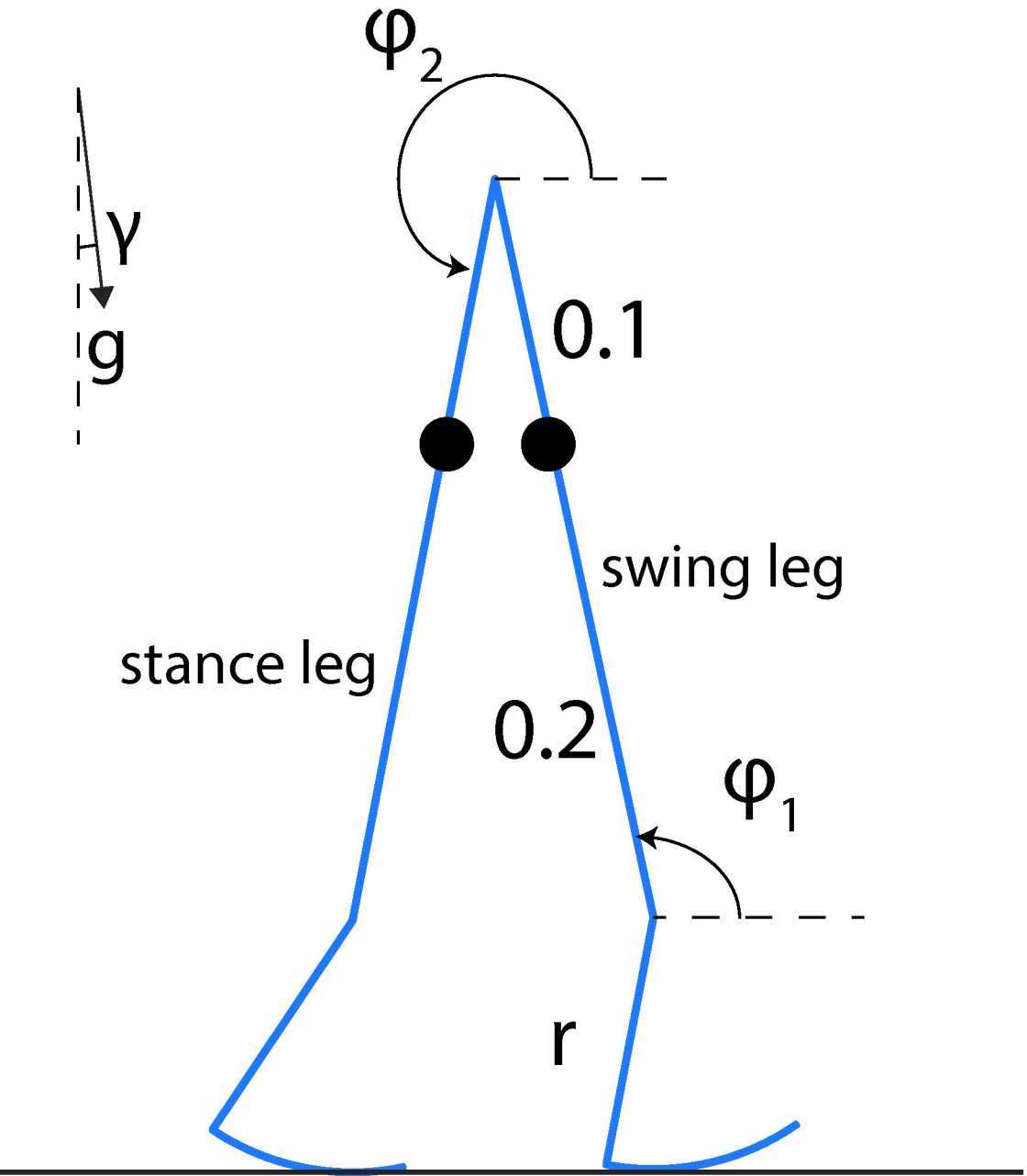
φ2
γ
g
0.1
swing leg
stance leg
0.2
φ1
r

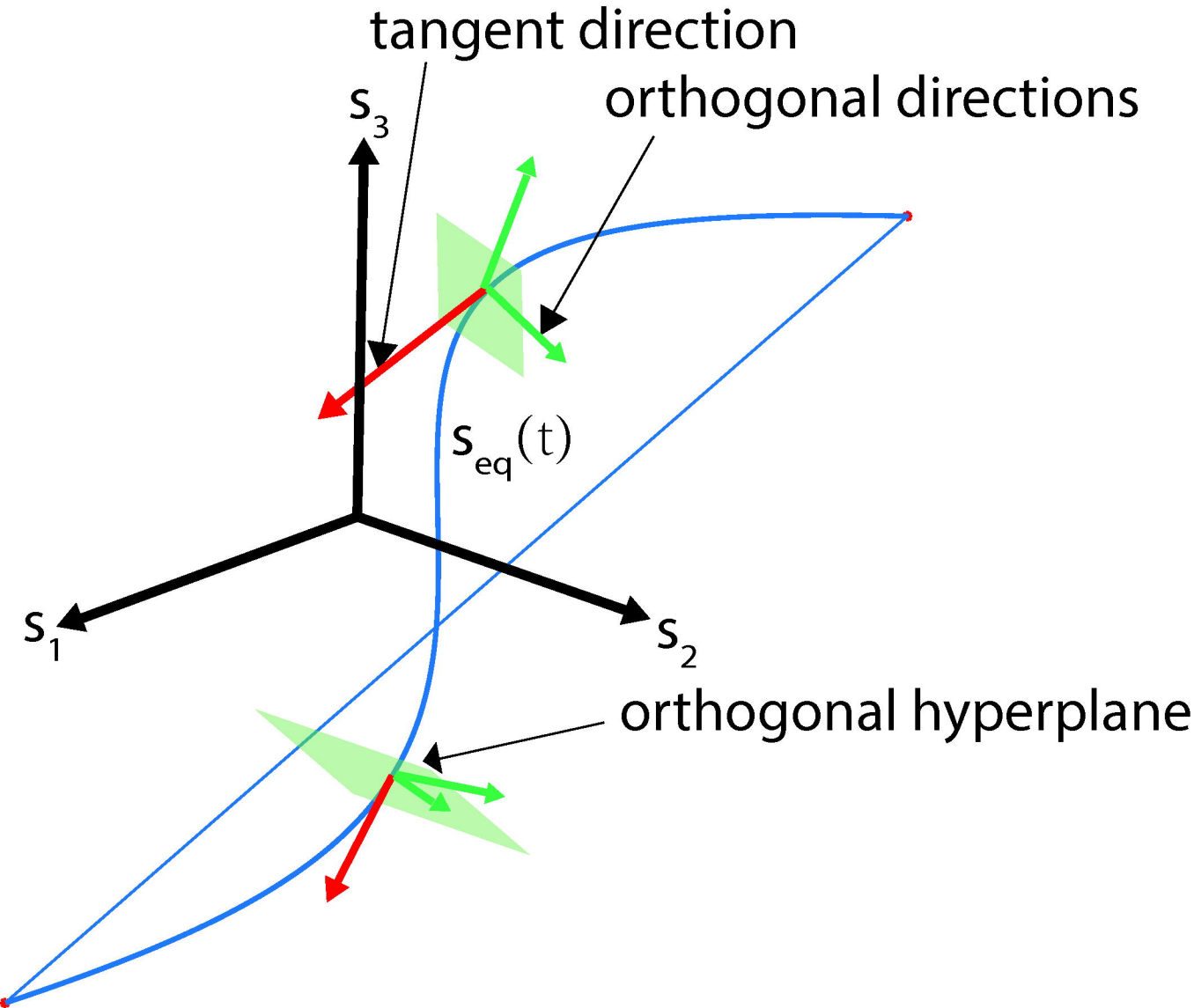
tangent direction
orthogonal directions
s_3
$s_{eq}(t)$
s_1
s_2
orthogonal hyperplane

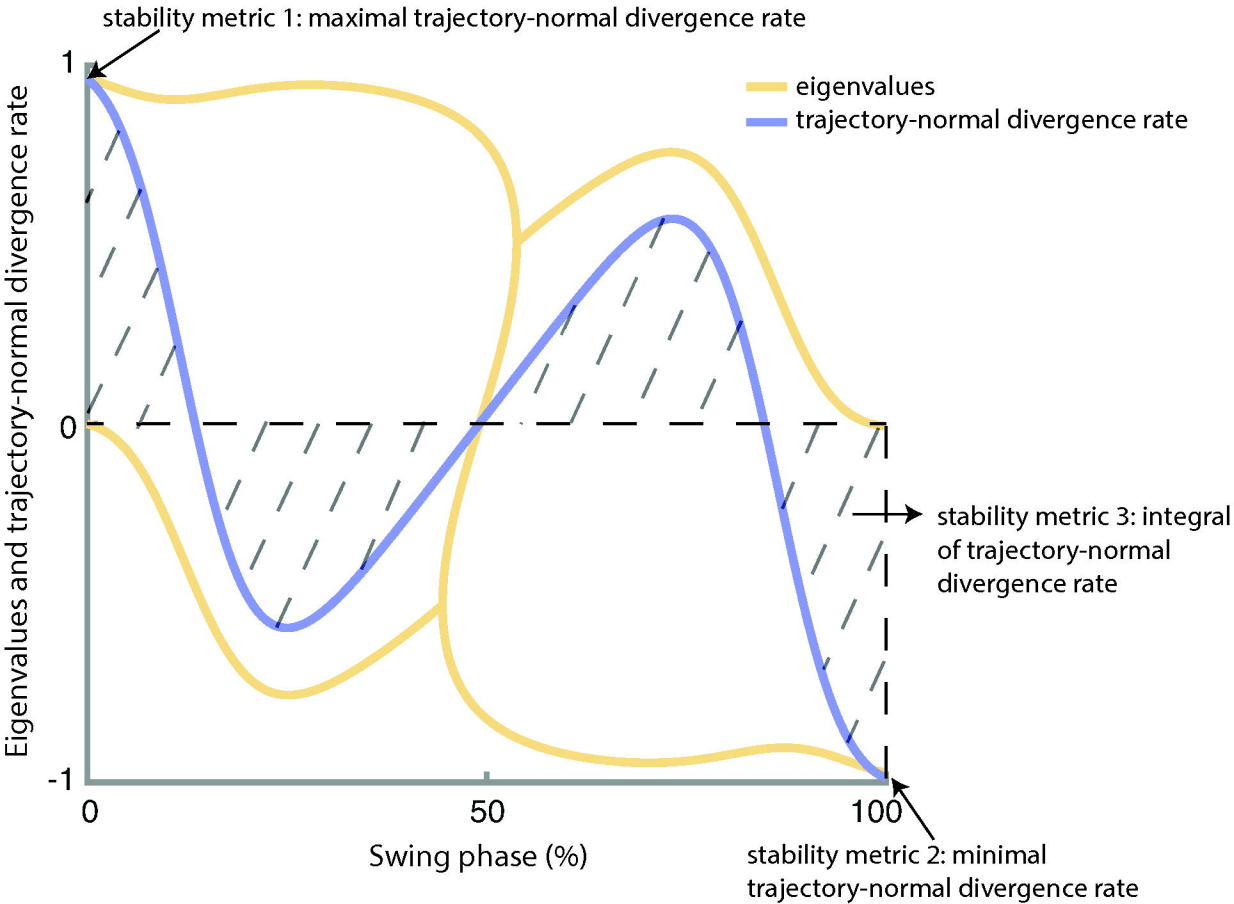
stability metric 1: maximal trajectory-normal divergence rate
eigenvalues
trajectory-normal divergence rate
stability metric 3: integral of trajectory-normal divergence rate
stability metric 2: minimal trajectory-normal divergence rate
Eigenvalues and trajectory-normal divergence rate
Swing phase (%)
1
0
-1
0
50
100

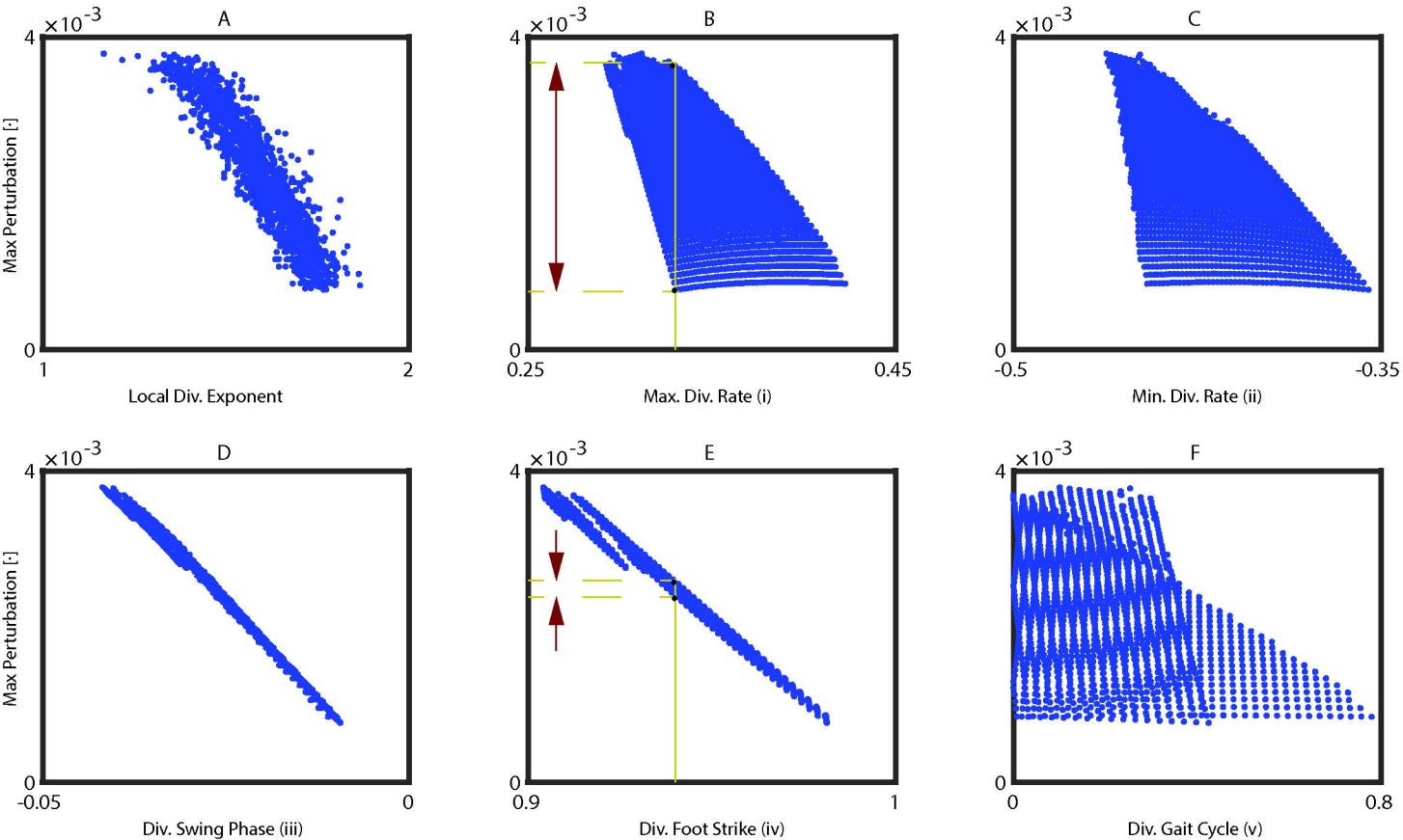
A
B
C
D
E
F
×10^-3
4
0
Max Perturbation [-]
1
2
Local Div. Exponent
0.25
0.45
Max. Div. Rate (i)
-0.5
-0.35
Min. Div. Rate (ii)
-0.05
0
Div. Swing Phase (iii)
0.9
1
Div. Foot Strike (iv)
0.8
Div. Gait Cycle (v)

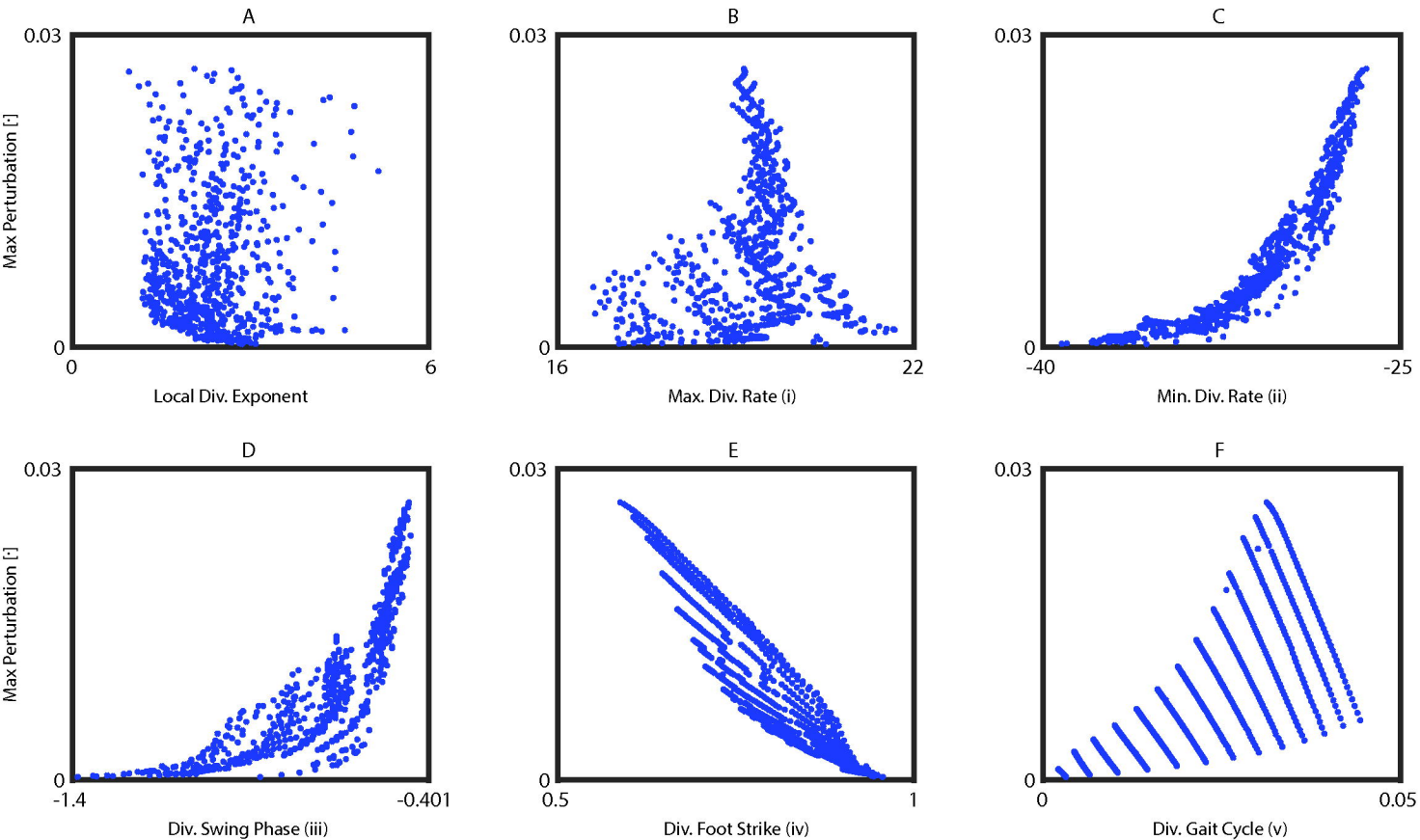
A
B
C
D
E
F
0.03
0
Max Perturbation [-]
0
6
Local Div. Exponent
16
22
Max. Div. Rate (i)
-40
-25
Min. Div. Rate (ii)
-1.4
-0.401
Div. Swing Phase (iii)
0.5
1
Div. Foot Strike (iv)
0
0.05
Div. Gait Cycle (v)

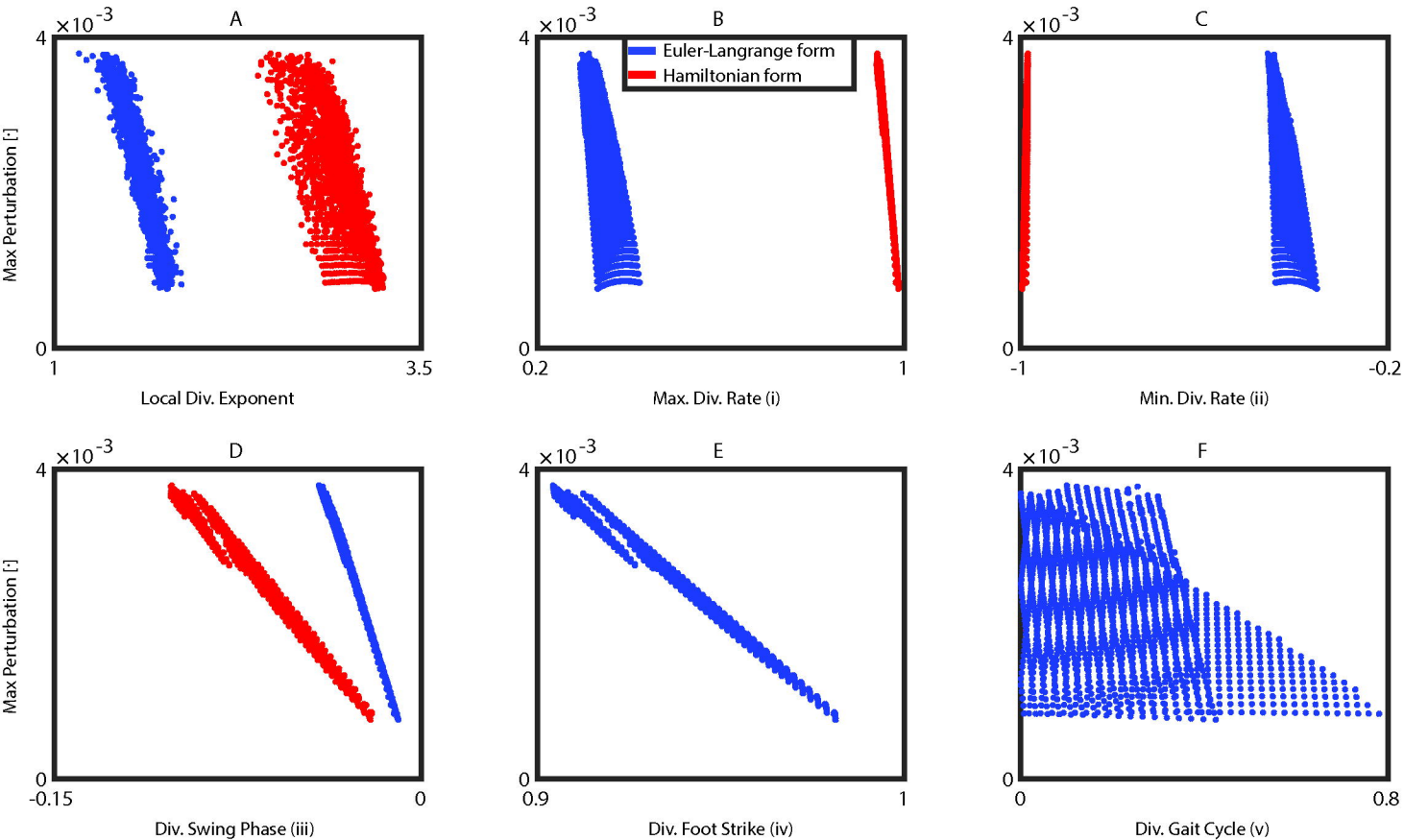
A
B
C
D
E
F
×10^-3
4
0
Max Perturbation [-]
Euler-Langrange form
Hamiltonian form
1
3.5
Local Div. Exponent
0.2
1
Max. Div. Rate (i)
-1
-0.2
Min. Div. Rate (ii)
-0.15
0
Div. Swing Phase (iii)
0.9
1
Div. Foot Strike (iv)
0
0.8
Div. Gait Cycle (v)

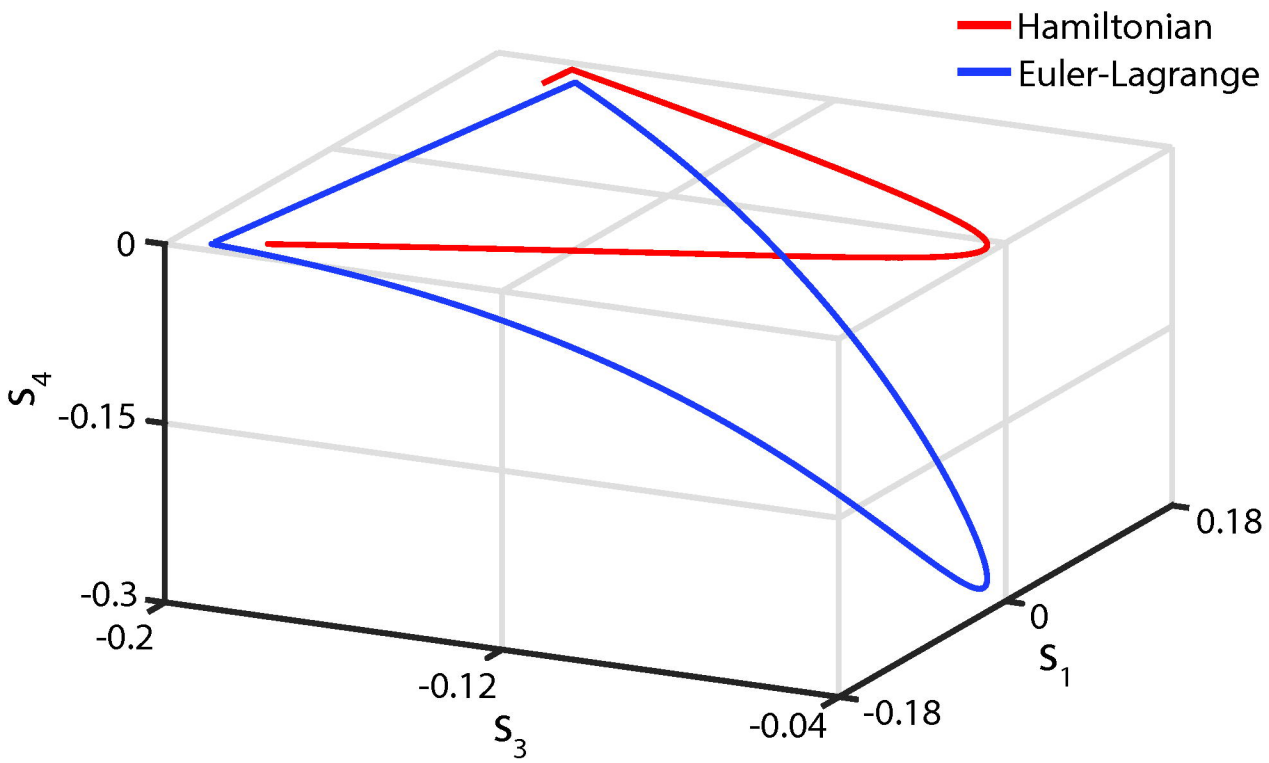
Hamiltonian
Euler-Lagrange
0
-0.15
-0.3
s_4
-0.2
-0.12
-0.04
s_3
-0.18
0
0.18
s_1

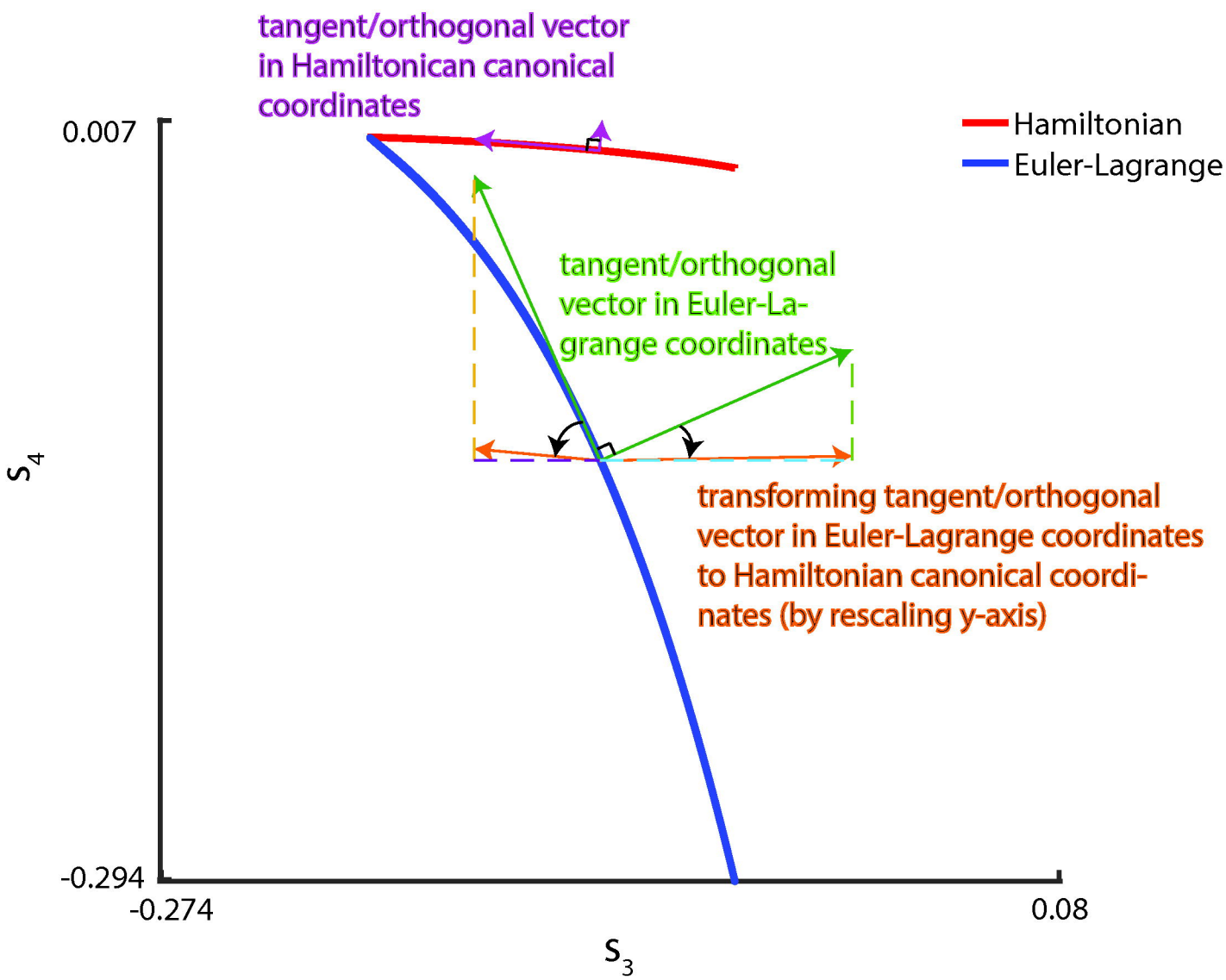
tangent/orthogonal vector in Hamiltonican canonical coordinates
0.007
Hamiltonian
Euler-Lagrange
tangent/orthogonal vector in Euler-La-grange coordinates
s_4
transforming tangent/orthogonal vector in Euler-Lagrange coordinates to Hamiltonian canonical coordi-nates (by rescaling y-axis)
-0.294
-0.274
0.08
s_3